PROCEEDINGS OF SCIENCE

Implementation of Silicon Detector Arrays in the UHV Environment of Storage Rings

B. Streicher[*a,b] **P. Egelhof**[b], **A. Glazenborg-Kluttig**[a], **S. Ilieva**[c], **N. Kalantar-Nayestanaki**[a], **H. Kollmus**[b], **T. Kröll**[c], **M. Lindemulder**[a], **G. May**[b], **M. Mutterer**[b], **C. Rigollet**[a], **M. von Schmid**[c], **M. Träger**[b],

*E-mail:*b.streicher@gsi.de

[a] *Kernfysisch Versneller Instituut, NL-9747 AA Groningen, Netherlands*

[b] *GSI Helmholtzzentrum für Schwerionenforschung GmbH, 64291, Darmstadt, Germany*

[c] *Technische Universität Darmstadt, 64289 ,Darmstadt, Germany*

The presented work focuses on the implementation of telescopic detector arrays in the UHV environment of a storage ring. The main advantage over the existing setups is the ability to place such telescopes in the storage ring vacuum without the need to enclose them fully in the standard pocket using stainless steel window. Our development utilizes the highly granular entrance Si-detector as an active window that separates the storage ring vacuum from the pocket vacuum where other detectors unsuitable for the UHV environment can be placed. Design and construction details of such detector system as well as results of the first performance tests are described in this contribution.

8th International Conference on Nuclear Physics at Storage Rings-Stori11,
October 9-14, 2011
Laboratori Nazionale di Frascati, Italy

[*] Speaker.

PoS(STORI11)072

1. Physics Motivation

The concept was conceived when designing the detection system for the upcoming project "EXotic nuclei studied in Light ion induced reactions (EXL)" [1] at the New Experimental Storage Ring (NESR) as a part of the future FAIR facility. By means of kinematically complete measurements in inverse kinematics, EXL provides for studying many physics phenomena in unstable nuclei (see Ref. [2] for the first feasibility tests of the concept). The crucial part of EXL is the 2π recoil particle detector ESPA. This detector array will consist of telescope-like segments which, depending on the different angular ranges, house pairs of double-sided silicon strip detectors (DSSDs) for particle tracking and identification, and the subsequent thick Si or Si(Li) detectors and/or CsI scintillator crystals for the spectroscopy and precise full-energy determination of high-energy particles. The innermost DSSDs are common for all the segments and will be arranged in a spherical configuration. The major technical challenge is to install a large number of detector channels with the correlated front-end electronics, connectors and cables, and possibly cooling circuits at the beam-target interaction region of the NESR where the need of an Ultra-High Vacuum (UHV) below the order of 10^{-10} mbar requires low-outgassing and bakeable materials. At the same time the physics program requires measuring some of the recoiling particles with the energies as low as possible, therefore separating the detector array in the stainless steal enclosure is not an option. For the implementation of all detectors in the NESR environment, a new differential pumping concept was envisaged [3] where the storage ring UHV is maintained inside the innermost sphere of DSSDs which is acting as a vacuum barrier to an outer volume, with less stringent constraint in vacuum quality, containing the subsequent layers of detectors and unbakeable and thus outgassing electronic components. Since the vacuum barrier serves at the same time the purpose of an active window it enables the detection of recoil particles varying from protons to alphas down to about 100 keV energy, as required for the measurement at low momentum transfer.

2. Technical Concept

The DSSD sensor with an active area of 19×19 mm^2 and thickness of 300 μm used in our prototype has 64 strips of 19 mm length on each side. The strips on the two sides are perpendicular to each other. This sensor was housed in the Printed Circuit Board (PCB) that was manufactured from aluminum nitride (AlN) ceramic. This material was chosen for its low outgassing, good dielectric properties, high thermal conductivity and thermal expansion coefficient close to that of silicon. The transmission mount design of the PCB is shown in Fig. 1. It has 16 printed gold signal lines for every side of the detector. The signal lines from the PCB side facing the UHV pass through the AlN material via laser-drilled holes covered with a glass layer to assure vacuum tightness. This ensures that the UHV side consists entirely of UHV compatible materials such as the AlN board with golden printed lines, the DSSD and the aluminum bonding wires all of which have low outgassing and can be subjected to baking. The DSSD sensor was hermetically glued in a laser-cut step, seen in the detail cut of Fig. 1, using a low-outgassing EPO-TEK H77 [4] two-component glue which has a total mass loss less than 0.06% at 200°C. The detector strips were manually bonded to the bonding pads printed on the PCB, grouping four neighboring channels to a single pad.

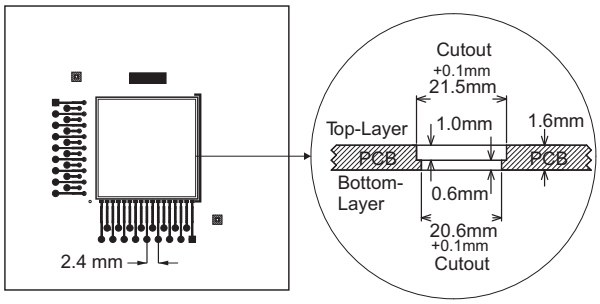

Figure 1: Layout of the printed circuit board made from AlN material. The two horizontal and two vertical rows of the signal pads are bonded to the n-side and the p-side of the DSSD, respectively (for clarity, the DSSD is not shown). The cross-sectional view on the right side shows a detail of an opening onto which the DSSD sensor is glued.

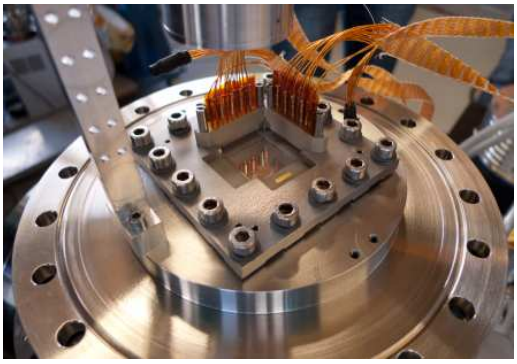

Figure 2: Photo of the test flange that separated the two vacuum chambers and onto which the ceramic PCB was mounted using the top frame. The α-source holder and PEEK connectors with spring pins are also visible.

Custom made connectors were manufactured using PEEK® material which is well machinable and can withstand the temperature required for the bake-out procedure. They were mechanically fixed on the stainless steel cover flange rather than on the PCB. The connection to the signal traces on the PCB was accomplished by spring-pin probes [5] that touched the circular printed pads on the PCB and, on the other side, were glued to the cable lines using EPO-TEK H22 conductive glue. The minimum contact area to the PCB and the thin walls of these tube-like probes minimize the heat transfer to the connector and subsequent cables during the bake-out process.

The idea of using DSSDs as a vacuum barrier to separate the storage ring vacuum from the auxiliary vacuum was realized in a small test vacuum chamber divided into two parts and separated by a custom machined CF150 flange with an opening of 4×4 cm^2 in the middle, as shown in Fig. 2. The PCB was installed over this opening using another steel top frame and two rings made of aluminum wires of 1.5 mm diameter. On each side of the PCB one ring was installed in order to minimize the mechanical forces acting on the PCB during the baking, however only the bottom one served the purpose of a vacuum seal. A small groove of 0.3 mm height was machined around the opening on the CF150 flange, as well as on the top frame, to hold both seals in place.

The top frame was tightened with 16 M5 screws using disc spring washers enabling one to press the PCB between the aluminum seals with a known force of 12 ± 2 N per mm of wire length. The top frame was situated on the Auxiliary Vacuum (AV) side and attached to it were the connectors to read both sides of the DSSD. The detector was tested using an ^{241}Am α source also mounted on the AV side in order to avoid its excessive heating by bake-out cycle. It was enclosed in an aluminum holder screwed onto the CF150 flange.

The vacuum test stand is schematically shown in Fig. 3. Each side was equipped with a TurboMolecular Pump (TMP) with a pumping speed of 250 l/s coupled through CF100 flanges. The pre-pump A was a combination of an oil-free membrane pump with a TMP. The combination was used as a booster for the next TMP. The pre-pump B was a rotary vane pump. First, both sides were pumped in parallel by pre-pump A with valves 1 and 2 opened and valve 3 closed. After reaching a vacuum of 5×10^{-3} mbar valve 2 was closed, valve 3 opened and both sides were

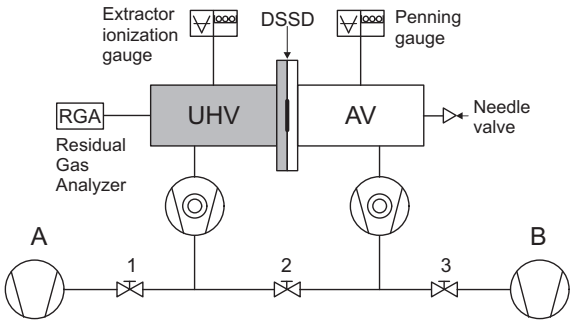

Figure 3: Block diagram of the setup for the differential vacuum test. The shaded part of the chamber was wrapped in a heating jacket and baked out at 150°C in order to reach UHV.

pumped separately using their own TMPs. In this configuration the only interplay between the two chambers was through the installed PCB holding the detector. After that the UHV side was gradually baked with heating jackets up to 150°C during a period of 2 days in order to remove water and other trace gases which were adsorbed on the surfaces of the chamber and the PCB-DSSD barrier. Following the bake-out the temperature was ramped down in one day to reach room temperature.

3. Measurements and Results

After the bake-out, on the UHV side the vacuum reached the value of 1.2×10^{-10} mbar, which was the limit of the installed TMP for the given conductance through a CF100 flange. The corresponding vacuum on the AV side was 2.2×10^{-7} mbar. Using the needle valve (Fig. 3) we introduced an artificial air leak on the AV side to observe its influence on the UHV side through the PCB-DSSD barrier. The results are shown in Fig. 4. Very stable vacuum conditions were maintained on the UHV side.

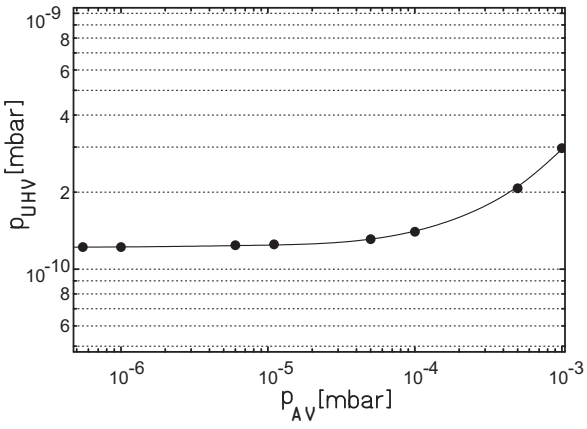

Figure 4: Dependence of the pressure on the UHV side on the AV side pressure influenced by an air leak artificially introduced through the installed needle valve.

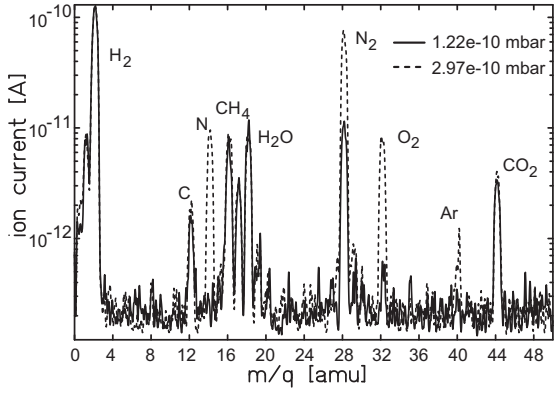

Figure 5: Outgassing spectra taken at the UHV side of the chamber with the residual gas analyzer. The solid curve shows the residual gas spectrum when no leak was present and the dotted curve the one after the leak at the AV side reached its maximum value.

While the pressure on the AV side increased due to the leak over a range greater than four orders of magnitude, the pressure on the UHV side increased by less than a factor of three, staying well within the achieved 10^{-10} mbar range. Thus, we have established that the DSSD, used as a differential vacuum barrier, can maintain a difference in the vacuum between both sides of the barrier of up to six orders of magnitude.

Outgassing spectra were measured on the UHV side with a residual gas analyzer for two cases: before the leak on the AV side was introduced and with a maximum leak. The results are shown in Fig. 5. The spectrum has the typical features of an air leak and it is free of organic compounds. The most pronounced increase was detected in molecular and atomic nitrogen, molecular oxygen as well as argon, which are the basic air constituents.

At the end of the bake-out and vacuum tests a measurement of the DSSD performance was done using injection of ^{241}Am α particles. The idea was to check whether the PCB-DSSD system can withstand the bake-out procedure and the mechanical forces introduced by the temperature change and to evaluate their influence on the spectroscopic performance. The injection from the n^+ side was chosen since the α source could not be placed in the baked environment of the UHV chamber. Because injection of α particles from the n^+ side results in a degraded resolution for our type of DSSD compared to injection from the p^+ side, only a basic functionality check was done proving that all 16+16 channels were fully operational. However, two supplementary measurements, one before and one after the bake-out and vacuum tests, were performed in a different non-UHV chamber using the p^+ injection to investigate the influence of the bake-out cycle on the DSSD performance. The moderate vacuum condition of $\sim 10^{-4}$ mbar, sufficient for such spectroscopy tests, were used in both measurements with no pressure difference between the two faces of the DSSD. The results show that the basic detector properties such as the detector leakage current, in our case of the order of few tens of pA, as well as signal rise time and amplitude after the preamplifier remained unchanged within the margin of the experimental error. Therefore, we claim that the DSSD characteristics were not influenced by the bake-out cycle and the energy resolution values for the p^+ injection achieved before and after the bake-out cycle coincide within the uncertainty of the measurement.

4. Future Perspectives

The EXL collaboration plans to perform the experiments with stable and close to stability radioactive beams such as ^{58}Ni and ^{56}Ni already at the present storage ring, as described in the accepted experimental proposal E105 for the existing storage ring at GSI. For this experiment planned at the end of 2012 we constructed a new detector of 64×64 mm^2 active area with 128 and 64 strips on p^+ and n^+ side, respectively, on a corresponding AlN PCB as seen in Fig. 6. The size and number of strips of this DSSD represent the detector adequate for the final EXL design. In order to guarantee the mechanical stability, to minimize sheer stress and to use even lower pressing power we intend to use high quality Helicoflex® [6] rings that lack the welded joint of the currently used aluminum rings, are very planar and have small and well-defined contact surface. The surface quality of the PCBs is also improved to have surface smoothness on the order of 0.5 μm and planarity of 50 μm compared to the guaranteed values of 4-6 μm and 250 μm, respectively, for the present PCB.

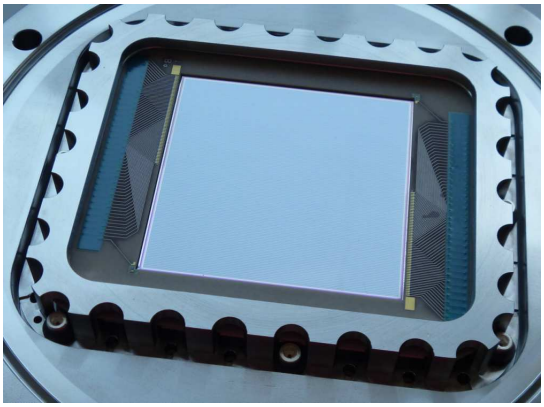

Figure 6: Clamped PCB of the 128×64 strip DSSD.

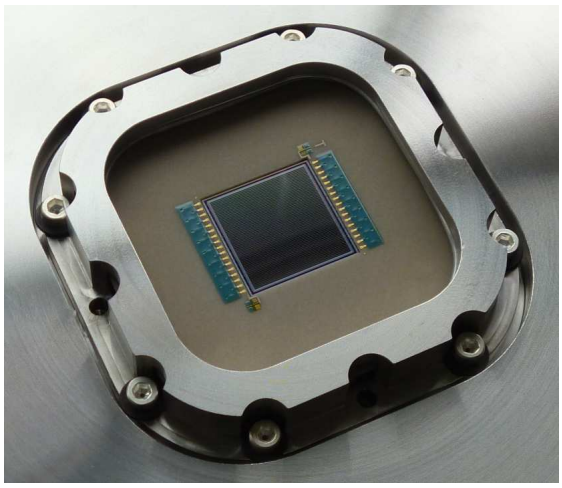

Figure 7: Clamped PCB for the improved version of the 64×64 strip DSSD.

In order to investigate the mechanical stability we started the new set of tests using the improved PCB for the 19×19 mm^2 DSSD shown in Fig. 7 and such tests will be done with the bigger 64×64 mm^2 strip DSSD of Fig. 6 as well. The first set of experiments will incorporate also Si(Li) detectors stacked as seen in Fig. 8 inside the AV of the pocket. Since the experimental chamber and the pocket on the outside have to be backed, the Si(Li) detectors must be cooled during this period to a reasonable temperature of about 50°C. This development still needs to be performed with respect to proper thermal simulations and also tested using a "dummy" Si(Li) detector to ensure both heating of the outside of the pocket and at the same time keeping the detector temperature at the reasonable value. This work should result in the final ESR pocket construction and tests by the middle of 2012.

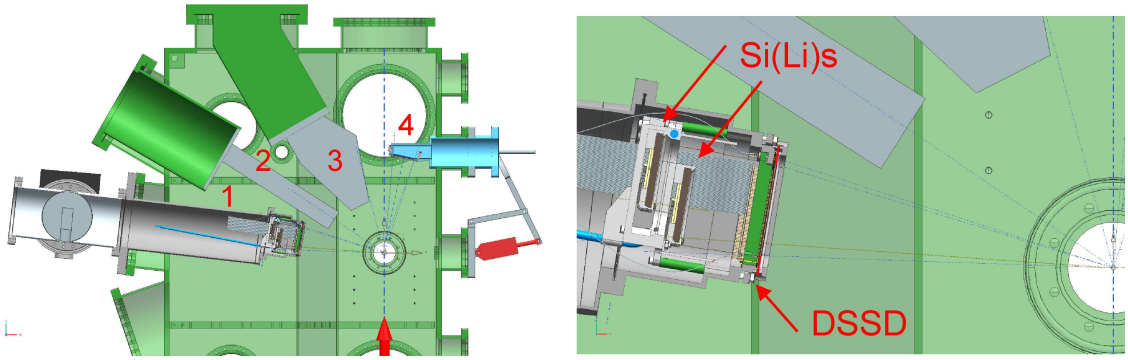

Figure 8: Schematic view of the ESR experimental chamber for the scaled-down version of the EXL project. On the left, the placement of various detector arrays is annotated 1-4. On the right, the closeup view of the assembly "1" is shown, currently under construction.

5. Conclusions

The aforementioned prototyping was done in the frame of R&D for the EXL project in order to insure that the experimental concept, namely using a stack of detectors in the UHV environment, is feasible. Our test results demonstrate the possibility of operating a differential vacuum system in the storage ring environment using DSSDs as a vacuum barrier. It was shown that the PCB-DSSD system withstands the bake-out cycle and the mechanical sheer stresses connected with the thermal expansion with unchanged spectroscopy performance, within the experimental errors. Chosen materials facing the UHV environment proved to be clean of any UHV disturbing contaminants. The achieved vacuum difference ranged over more than six orders of magnitude with the vacuum on the UHV side staying well within the 10^{-10} mbar range, which is an acceptable vacuum for the interaction region with internal target at the storage ring.

It should be noted that the concept of this development can be potentially applied outside of the EXL project for experiments at storage rings requiring the usage of DSSDs in UHV. Due to the fact that the entrance detector serves the purpose of an active window, telescope-like detector configurations used in the UHV can measure low-energy particles of about 100 keV as well as penetrating particles with energies of several hundreds of MeV stopped in subsequent detectors.

This work was supported in part by BMBF (06DA9040I) and HIC for FAIR.

References

[1] **EXL home page:** http://www.rug.nl/kvi/Research/hnp/Research/EXL/index

[2] H. Moeini, S. Ilieva *et al.*, Nucl. Instrum. Methods. Phys. Res. A, 634 (2011) 77-84

[3] B. Streicher *et al.*, Nucl. Instrum. Methods. Phys. Res. A 654 (2011) 604-607

[4] **Glue producer:** http://www.epotek.com

[5] **Spring pin producer:** http://www.idinet.com

[6] **Seal producer:** http://www.helicoflex.com